ELSEVIER

Journal of Alloys and Compounds 402 (2005) 170–185

Journal of ALLOYS AND COMPOUNDS

www.elsevier.com/locate/jallcom

Experimental study of the ternary magnesium–aluminium–strontium system

M.A. Parvez [a], M. Medraj [a,*], E. Essadiqi [b], A. Muntasar [c], G. Dénès [c]

[a] *Mechanical Engineering Department, Concordia University, 1455 de Maissonneuve Blvd H549, Montreal, PQ, Canada H3G 1M8*
[b] *CANMET-MTL, Ottawa, Canada*
[c] *Chemistry Department, Concordia University, Montreal, Canada*

Received 29 March 2005; received in revised form 25 April 2005; accepted 26 April 2005
Available online 27 July 2005

Abstract

The phase diagram of the ternary magnesium–aluminium–strontium (Mg–Al–Sr) system has been investigated with 22 different alloys by DSC, XRD and metallography. Liquidus temperature and enthalpy were determined. Al_4Sr and (Mg) were found to be the dominating phases in the investigated alloys. Four new phase fields have been identified; the new phases were tentatively designated as τ_1, τ_2, τ_3 and τ_4 and may be ternary intermetallics or solid solutions. Some peak positions of τ_1 corresponded well with the newly reported ternary compound $Al_3Mg_{13}Sr$. The identified phases in the as-cast condition were found consistent and thermodynamically stable with the post-DSC sample ($25 \leftrightarrow 700\,^{\circ}C$) in the investigated alloys. Two ternary eutectic transformations have been observed. The experimental results were compared with the pertinent thermodynamic findings. A considerable discrepancy in the solid-phase transformation temperature was observed. Predicted phases by the thermodynamic calculation do not agree with the present XRD results for nine samples, which suggests that this system should be remodeled.

Keywords: Mg–Al–Sr ternary system; Phase diagram; Thermal analysis; X-ray diffraction; Microstructure; Thermodynamics

1. Introduction

Magnesium-based alloys are particularly attractive for transportation applications for weight reduction and higher fuel efficiency [1,2]. However, magnesium alloys face a challenge at higher temperature application because of their restricted creep properties. In recent years, magnesium–aluminium–strontium (Mg–Al–Sr) alloy system has emerged as potential for heat-resistant Mg-alloys [3]. Recently, Noranda developed alloys based on Mg–Al–Sr system, which will be used by BMW for the manufacturing of die-cast engine blocks.

Within the ternary Mg–Al–Sr system, there is a huge amount of possibilities to select alloy compositions. Wrought magnesium, particularly in the form of sheet, represents a tremendous growth opportunity in the application of magnesium. The phase relations and phase stability under given conditions can be better understood using equilibrium diagrams. Hence, it is important to make a detailed and complete study of the Mg–Al–Sr phase diagram.

To date, little effort has been made to construct the phase relationships of Mg–Al–Sr system. The published experimental works on the phase equilibria of Mg–Al–Sr system are self-contradictory. Prince and Nikitina [4] summarized the work done on the Mg–Al–Sr system. The experimental work on the phase equilibria of the Mg–Al–Sr system primarily originated by Makhmudov et al. [5–9]. However, inconsistency was noticed between their works, which were published from 1980 to 1982. The 400 °C isothermal section shows a triangulation involving (Mg), $Mg_{17}Sr_2$ and γ phase.

* Corresponding author. Tel.: +1 514 848 2424x3146; fax: +1 514 848 3175.
E-mail address: mmedraj@encs.concordia.ca (M. Medraj).
URL: http://www.me.concordia.ca/~mmedraj.

0925-8388/$ – see front matter © 2005 Elsevier B.V. All rights reserved.
doi:10.1016/j.jallcom.2005.04.173

But it seems unlikely, as the thermodynamic stabilities of these compounds are low as compared to Al_4Sr and Al_2Sr. Makhmudov et al. also reported a ternary compound with stoichiometry of $Al_{34}Mg_6Sr_{60}$ (Al_6MgSr_{10}), which is different from the earlier reported X compound. The solubility limits for the binary compounds determined by Makhmudov et al. [8] do not agree with the 400 °C isothermal section given by Makhmudov et al. [7] in 1981. Prince and Nikitina [4] developed a tentative liquidus surface by using the experimental results of Makhmudov et al. [6–9] with some disagreements in identifying the invariant points. Baril et al. [10] recently investigated four samples of Mg–Al–Sr system experimentally in the Mg-rich region and tentatively designated a ternary phase as $Al_3Mg_{13}Sr$. The stoichiometry is not yet clearly identified and the chemical composition is not compatible with the ternary compound $Al_{34}Mg_6Sr_{60}$ reported by Makhmudov et al. [7]. Chartrand and Pelton [11] critically reviewed and calculated the thermodynamic properties of the Mg–Al–Sr ternary and related binary subsystems. No ternary terms were added to the thermodynamic model due to the uncertainties related to the existence, stability, homogeneity range and the melting and decomposition temperature of the ternary compounds. In 2003, Koray [12] calculated the liquidus projection of the ternary Mg–Al–Sr system that is very similar to Chartrand and Pelton's [11] calculation, except for the narrower phase field of Mg_2Sr. The calculated phase diagram exhibited substantial disagreement with the experimental data. The extended solubilities between solid phases were not considered in the thermo dynamic assessments. The 400 °C experimental isothermal section also shows the triangulations involving Al_4Sr in equilibrium with $Mg_{17}Sr_2$, $Mg_{23}Sr_6$ and Mg_2Sr; however, these compounds are calculated to be in triangulation with Al_2Sr. From these discrepancies, it is believed that this thermodynamic evaluation of the ternary system should be considered as tentative. Furthermore, in the experimental work of Makhmudov et al. [8], the binary compound $Mg_{38}Sr_9$ was not included in their Mg–Al–Sr phase diagram. In 2004, Liu et al. [13] reported the potential existence of Al_3Sr_8 and Al_5Sr_4 compounds that will definitely alter the thermodynamic optimization of Mg–Al–Sr ternary diagram. A considerable discrepancy among the published results and very few experimental data demands new investigation for this system, and hence, a detailed investigation by DSC, XRD and metallography methods was carried out.

2. Experimental

Twenty-two samples were chosen by critical assessment of the experimental and thermodynamic datasets that are available in the literature. Table 1 shows the different groups with the number of samples and their phase fields that were predicted by thermodynamic modeling. Special attention was focused on the Mg-rich corner because of the interest in the Mg alloys. Since, Al_4Sr gives the thermodynamic stability to Mg–Al–Sr-based alloys, samples containing this phase were also chosen. This will help in determining the extent of the Al_4Sr phase field. In addition, two samples at the eutectic points reported by Makhmudov et al. [11] were prepared.

Table 1
Samples in different phase fields

Group (no.)	Sample no.	Predicted phases
1	1, 2, 3, 4, 5, 6, 7, 8, 9	(Mg) + Al_4Sr + γ
2	10, 11, 12, 13, 14	(Mg) + Al_2Sr + Al_4Sr
3	15, 16, 17	Al_4Sr + γ + β
4	18, 19, 20	(Al) + Al_4Sr + β
5	21, 22	(Mg) + Al_2Sr + $Mg_{17}Sr_2$

Mg–Al–Sr ternary diagram with the investigated compositions in weight percentage are given in Fig. 1. The nominal sample compositions remained in very close proximity with the actual composition. Moreover, the thermodynamic prediction of the liquidus temperature for the nominal and actual compositions was almost the same for most of the samples. In preparing the Mg–Al–Sr-based alloys, magnesium of 99.8 wt.%, aluminum of 99.9 wt.% and strontium of 99 wt.% were used. The charge was melted in a graphite crucible in an induction-melting furnace under argon with 1% sulfur hexafluoride (SF_6) to protect the melt from oxidation and followed by slow cooling. The actual chemical composition was measured quantitatively by ICP atomic emission spectrometry. The loss in total mass was below 2% for most of the samples.

Thermal investigation of this system was performed using a Setaram Setsys DSC-1200 instrument. Temperature calibration of the DSC equipment was done using pure Mg and Al. The samples were cut and mechanically polished to remove any possible contaminated surface layers. After-

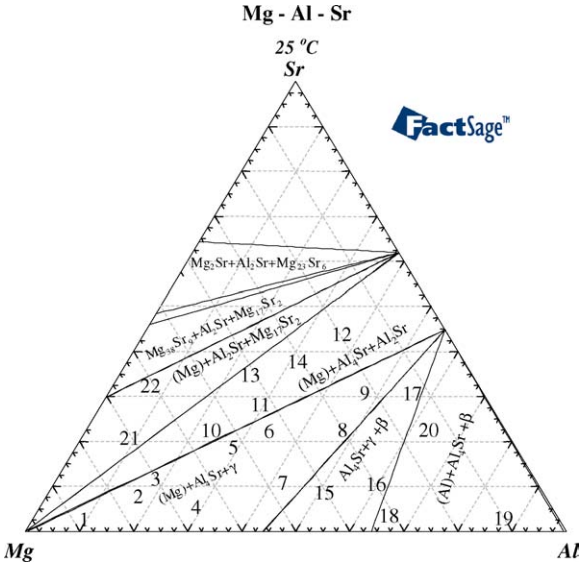

Fig. 1. Mg–Al–Sr ternary isothermal section at 25 °C showing investigated compositions in wt.%.

wards, they were cleaned with acetone, and placed in a graphite crucible with a lid cover to contain Mg vapors and protect the apparatus. To avoid oxidation, multiple evacuations, followed by rinses with pure argon, were done. The DSC measurements were carried with heating and cooling rates of 5 °C/min. Slower heating rates were tried and were not found to reveal any other thermal arrests. The weight of the sample was 40–50 mg. During the calibration, it was made certain that the geometrical dimensions and the surface quality did not show any visible effects on DSC spectra. The reproducibility of every measurement was confirmed by collecting the data during three heating and cooling cycles. More details on the interpretation of the DSC experiments were reported in our previous works [14,15]. The estimated error between the repetitive heating and cooling is ±1 °C or less. Temperatures along with enthalpies corresponding to various thermal events were obtained. However, the solidification behavior can be revealed much better with the cooling scans. On heating, onset temperature was used for invariant reactions, while peak maximum was used for phase field boundaries. On cooling, onset temperature was used for both the invariant reactions and the phase field boundaries.

Phase identification was carried out by X-ray diffraction (XRD) with a Philips diffractometer (Cu Kα radiation) equipped with a PW 1050/25 focusing gonimometer with steps 0.02° of 2θ diffraction angle and 1 s exposure time. All the twenty-two samples were investigated in the powder form in the as-cast condition at room temperature. For the calibration of the X-ray diffractometer, powder was made from pure Mg supplied by Noranda, and diffraction patterns were obtained and compared with the literature. The relative peak intensity and the position matched completely. PowderCell 2.3 [16] was used to calculate the diffraction patterns for different phases and to identify their peaks [17]. The patterns were checked for known oxide phases, such as MgO, Al_2O_3 and $MgAl_2O_4$, for any possible oxide formation.

Microstructural observations were made using optical microscope (Olympus BX60M). The samples were etched using 1 vol% nital solution (HNO_3 in ethanol) for a short period of time (∼5 s) to prevent dissolving of the Mg grains.

Furthermore, to assure the homogeneity, the samples were taken from different locations in the castings, and identical phase transformations using DSC, were observed. Also, the melting enthalpy of these samples was very similar. Morphology of the same compositions at different locations from the castings were observed and found similar. The microstructure in the post-DSC samples was also observed for five samples and compared with the as-cast condition. Although the grains' morphology and the network nature of the grain boundary experienced some changes, the phase types remain the same after the DSC experiment.

Phase assemblage diagrams and vertical sections have been drawn from the database provided by Chartrand and Pelton [11]. Phase assemblage diagrams show the relative amount of each phase and formation and decomposition temperatures. Vertical sections are calculated, and used to obtain the phase boundaries and the associated temperatures, which are compared with the DSC signals.

3. Results and discussion

3.1. Samples in (Mg) + Al_4Sr + γ phase field

Nine samples have been studied in the (Mg) + Al_4Sr + γ phase field, as shown in Fig. 1. DSC spectra of sample 1 with heating and cooling runs are shown in Fig. 2(a). The onset temperature, peak temperature, melting temperature and the melting enthalpy were registered. There are two peaks during heating that were also encountered during cooling. Similar results were observed in all three heating and cooling cycles. It can be seen from this figure that there is a temperature difference between the heating and cooling patterns; however, the maximum temperature difference of the observed signals between two repetitive heating or cooling runs were below 3 °C. During heating of this sample, two thermal arrests, corresponding to the invariant reaction at 527 °C and the univariant reaction at 605 °C, were registered. For this sample, the liquidus temperature was observed during cooling and found to be 609 °C.

The experimental results were compared with the thermodynamic calculations to confirm the transformation temperature along with the associated reaction. For this purpose, the vertical section was calculated using FactSage [18] and the database developed by Chartrand and Pelton [11]. Fig. 2(b) shows the calculated vertical section of sample 1 (3.32 wt.% Sr, 87.29 wt.% Mg and 9.39 wt.% Al) with DSC signals from the cooling curve. It can be observed that the liquidus temperature matched well with the experimental values. However, the transformation temperature predicted by the thermodynamic modeling at 222 °C was not observed in the DSC signals. Slower heating rate at 2 °C/min also did not reveal any signal at this temperature.

XRD was used to identify the phases in the studied samples at room temperature. The peaks are identified by markers given in the legend of each figure. In sample 1, two phases, (Mg) and Al_4Sr, were identified positively in the diffraction pattern. It can be seen from Fig. 2(c) that this sample is composed of a very little volume of γ at room temperature, but the number of peaks and the peak intensity are not enough to identify it positively. Shifting of Al_4Sr peaks to lower diffraction angles suggests that solid solubility between Mg and Al_4Sr might exist. (Mg) peaks are identified as a hexagonal unit cell (space group $P6_3/mmc$, $a = 3.1210$ Å and $c = 5.1581$ Å), while Al_4Sr and γ were identified using a tetragonal and cubic unit cell (space group $I4/mmm$, $a = 4.459$ Å and $c = 11.0700$ Å) and (space group $I43m$, $a = 10.5438$ Å), respectively [19]. Baril et al. [10] reported that the γ phase was not observed in an alloy with the chemical composition of 1.95 wt.% of Sr, 93.05 wt.% of Mg and 5.0 wt.% of Al, which is close to this sample. This

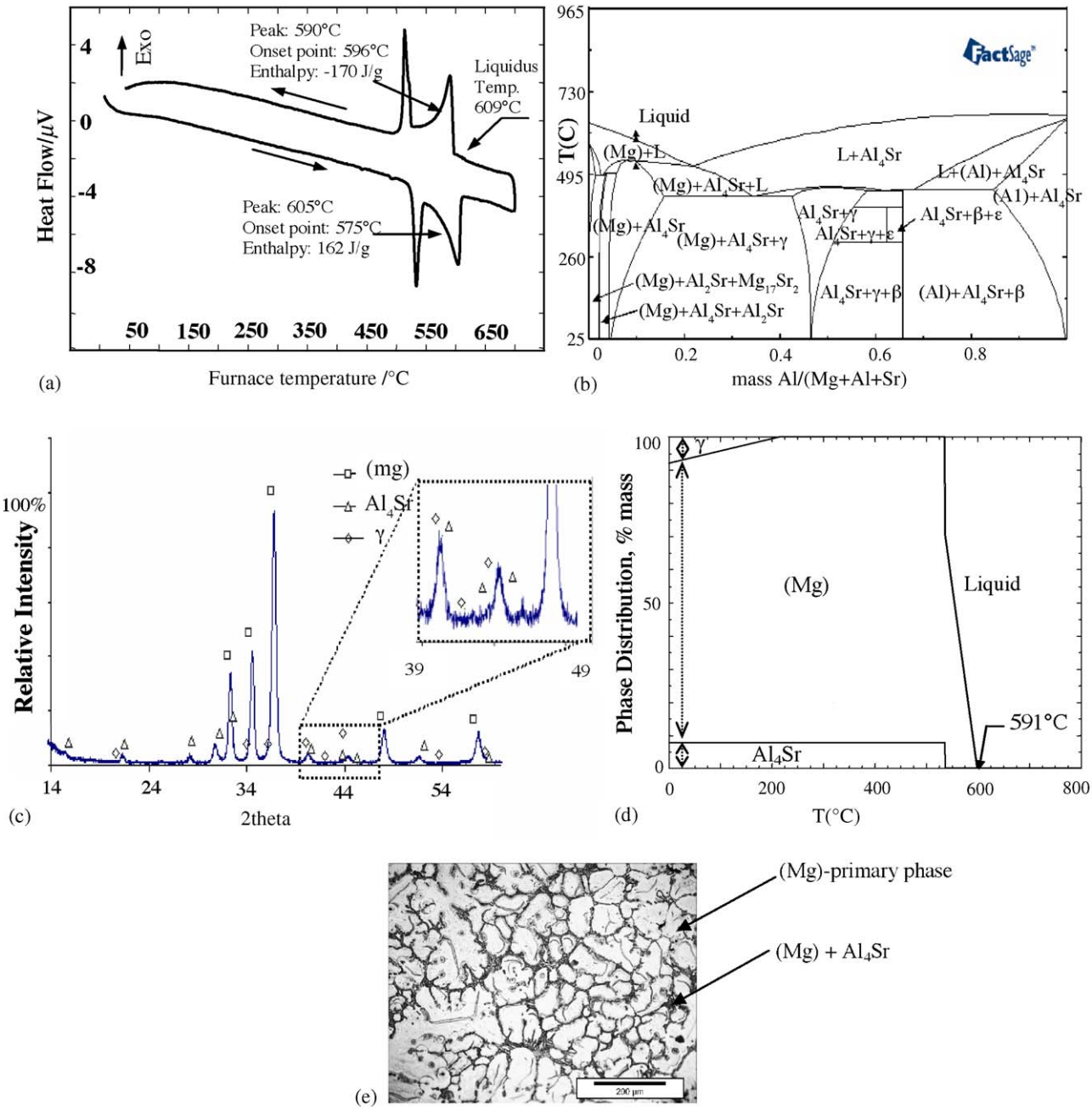

Fig. 2. (a) DSC spectra of sample 1 (3.32/87.29/9.39, Sr/Mg/Al, wt.%) during heating and cooling, (b) calculated vertical section at constant 3.32 wt.% Sr with DSC signals from cooling curve of sample 1, (c) XRD pattern of sample 1, (d) phase assemblage diagram of sample 1, and (e) optical micrograph of sample 1.

information along with some more samples in this Mg-rich region can be used to setup a window to identify the possible creep resistant alloy for the end user.

Fig. 2(d) shows the phase assemblage diagram of sample 1 (3.32 wt.% Sr, 87.29 wt.% Mg and 9.39 wt.% Al), where the relative mass versus temperature is calculated. The proportion of each phase at any temperature of interest can easily be interpreted from this figure. For instance, at 25 °C, 100 g of the overall material consists of 7.5 g of Al_4Sr, 7.5 g of γ and 85 g of (Mg). Moreover, Fig. 2(d) shows that while cooling this sample from the melt, (Mg) solidifies first, followed by Al_4Sr, and then γ. The proportion of each phase for this sample has been reflected in terms of peak intensity in the diffraction pattern. Since Sr has higher atomic weight, for Al_4Sr, higher peaks were observed compared to γ.

Fig. 2(e) shows the optical micrograph of sample 1. The primary (Mg) grains are surrounded by the interconnected network of the grain boundary phase. The grain boundary phase is formed during the eutectic solidification process, and thus, having a lamellar-type morphology. Baril et al.

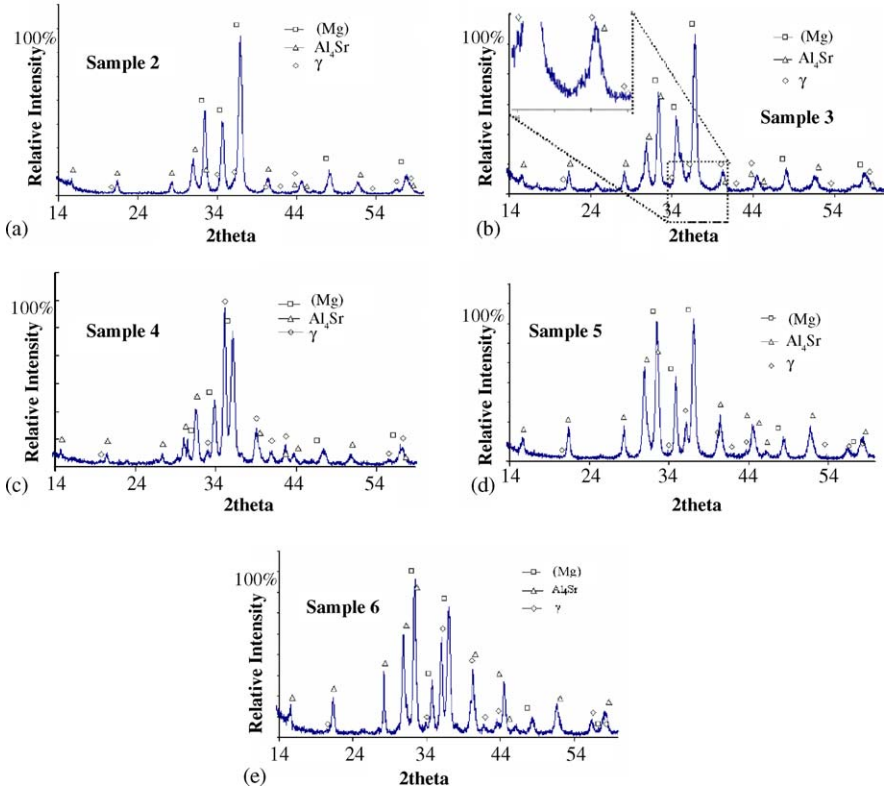

Fig. 3. XRD patterns of samples (a) 2 (8.65/76.15/15.20, Sr/Mg/Al, wt.%), (b) 3 (7.09/74.82/18.09, Sr/Mg/Al, wt.%), (c) 4 (6.88/65.45/27.67, Sr/Mg/Al, wt.%), (d) 5 (22.48/48.57/28.95, Sr/Mg/Al, wt.%), and (e) 6 (22.53/43.75/33.72, Sr/Mg/Al, wt.%).

[10] found Al_4Sr in the lamellar eutectic morphology in an alloy quite close to this sample. However, γ phase is difficult to reveal in the micrograph because of its small relative amount.

Fig. 3 shows that samples 2–6 have been identified positively with two phases (Mg), Al_4Sr, and a very small volume fraction of γ. This is consistent with the thermodynamic calculations, as shown in Fig. 4. Fig. 5 shows the microstructures of these samples. It can be seen from Fig. 4(c) and (d) that an increase in the content of Al_4Sr, predicted by the thermodynamics, has been reflected in the micrographs of samples 4 and 5. In samples 4 and 5, Al_4Sr precipitated first at 591 °C and then 648 °C, respectively, when cooling from the melt, as can be seen in Figs. 4(c) and (d). Furthermore, sample 4 was reported as a ternary eutectic by Makhmudov et al. [8]. However, the DSC spectra and phase assemblage diagram show that this sample is not eutectic. If it were ternary eutectic, all the three phases should have precipitated at the same temperature and DSC spectra should have been registered with a single peak. It can be seen from the micrographs (Fig. 5(c) and (e)) that Al_4Sr is the primary phase. In samples 4 and 6, the smaller lighter phase as seen in Fig. 5(c) and (e), has been tentatively designated as γ phase. It is not possible to identify the phases of sample 3 due to the very fine structure, as shown in Fig. 5(b), that requires higher magnification than the optical microscope.

DSC measurements and calculated thermal arrests for the samples 1–6 are presented in Table 2. It can be seen from this table that the thermodynamic calculation could not accurately predict all the transformations that have been measured by the DSC. Besides, the lower transformation temperature was not encountered in the DSC signals even when the samples were investigated at a lower scanning rate. Fig. 6 shows a comparison between the measured liquidus temperature obtained by the DSC experiments and predicted by the thermodynamics, which shows good agreement except for sample 4.

In this phase field, samples 7–9 were identified positively with Al_4Sr and γ using XRD. Some other distinct peaks that are not associated with the known phases in the Mg–Al–Sr system have been observed. There is no crystallographic information regarding any stable ternary compounds available in the literature. Some of the peaks of the XRD pattern for these samples did match well with a ternary compound tentatively designated as $Al_3Mg_{13}Sr$, and reported by Baril et al. [10]. However, the crystal structure of $Al_3Mg_{13}Sr$ is still unknown. Therefore, these peaks were tentatively designated as τ_1, which may be a new ternary compound or a ternary solid solution. It is very important to note that these distinct peaks appear in the XRD patterns of samples 7–9 in a similar fashion, as can be seen in Fig. 7. In the phase field of (Mg) + Al_4Sr + γ, Al_4Sr was found to be the dominating phase for most of the samples.

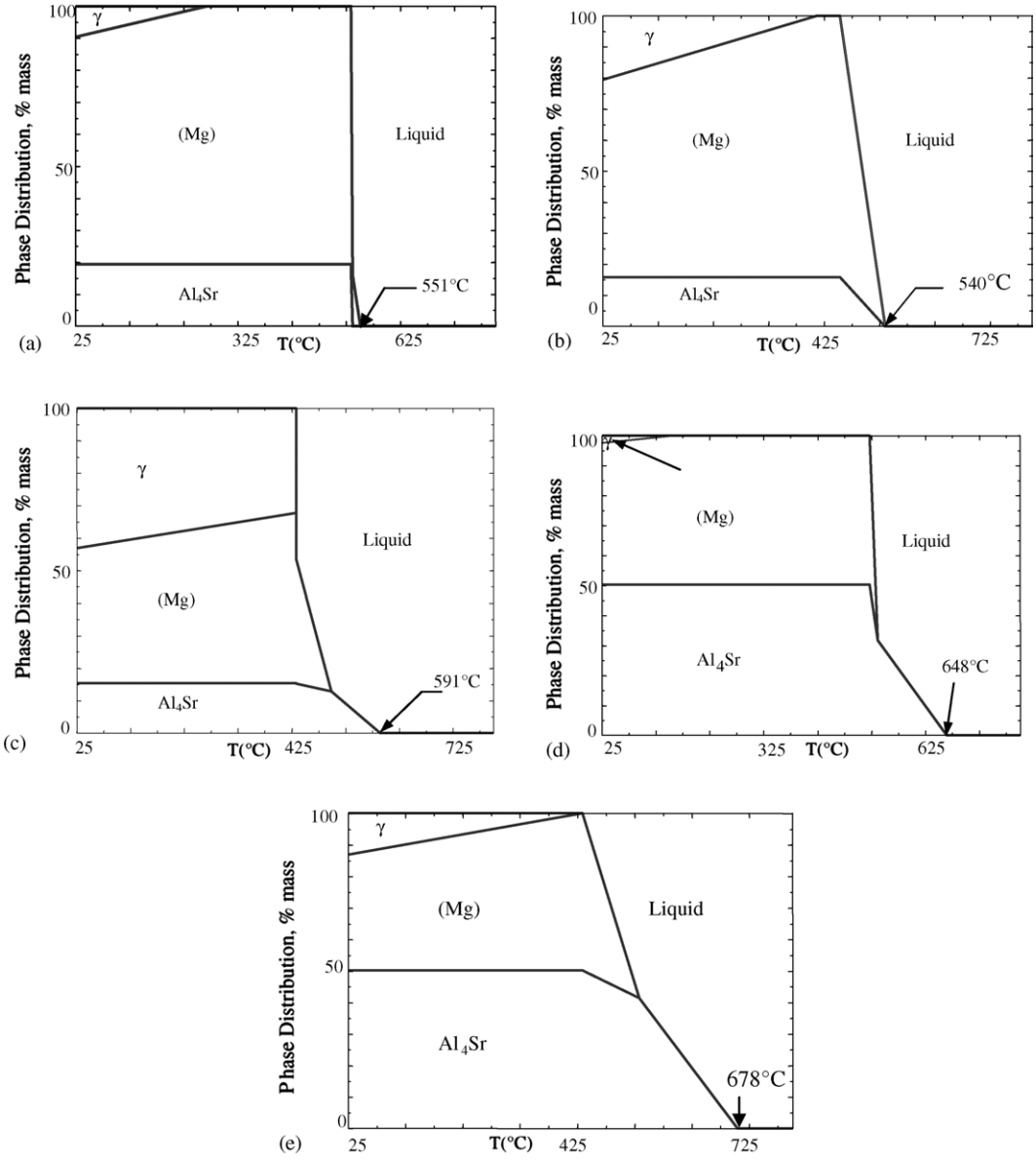

Fig. 4. Phase assemblage diagram of samples (a) 2, (b) 3, (c) 4, (d) 5, and (e) 6.

Table 3 summarizes the DSC measurements of these samples in relation to the results from thermodynamic modeling. The thermodynamic calculation was made to check the temperature of liquidus and the reaction between the phases. In all the three samples, the exothermic reaction starts at similar temperature 444–445 °C. The liquidus temperature for samples 8 and 9 could not be registered. It was observed from the phase assemblage diagram, shown in Fig. 8, that the samples are mainly composed of γ and Al_4Sr, which have been identified positively by XRD.

Fig. 9 shows the optical images of the microstructure of samples 7–9. The micrographs led to the conclusion that these remarkable plate-like structures are Al_4Sr, as it appeared in different samples in an identical morphology, and supported by the investigation conducted by Makhmudov et al. [6]. It is the primary phase in these alloys, as can be seen from the phase assemblage diagrams (Fig. 8).

3.2. *Samples in (Mg) + Al_4Sr + Al_2Sr phase field*

Five samples, as shown in Fig. 1, were studied in this phase field. In samples 10 and 11, (Mg) and Al_4Sr were identified in the diffraction patterns, as shown in Fig. 10(a) and (b). In contrast, XRD pattern of sample 12 was identified with Al_2Sr and Al_4Sr. Al_2Sr was identified using a rhombic unit cell (space group $Fd3m$, $a = 8.325(5)$ Å) [19]. However, the distinct peaks that are not associated with any of the known phases in the Mg–Al–Sr system, appeared in identical manner in all these three samples. And the new peaks may belong to a ternary compound or solid solution and tentatively designated

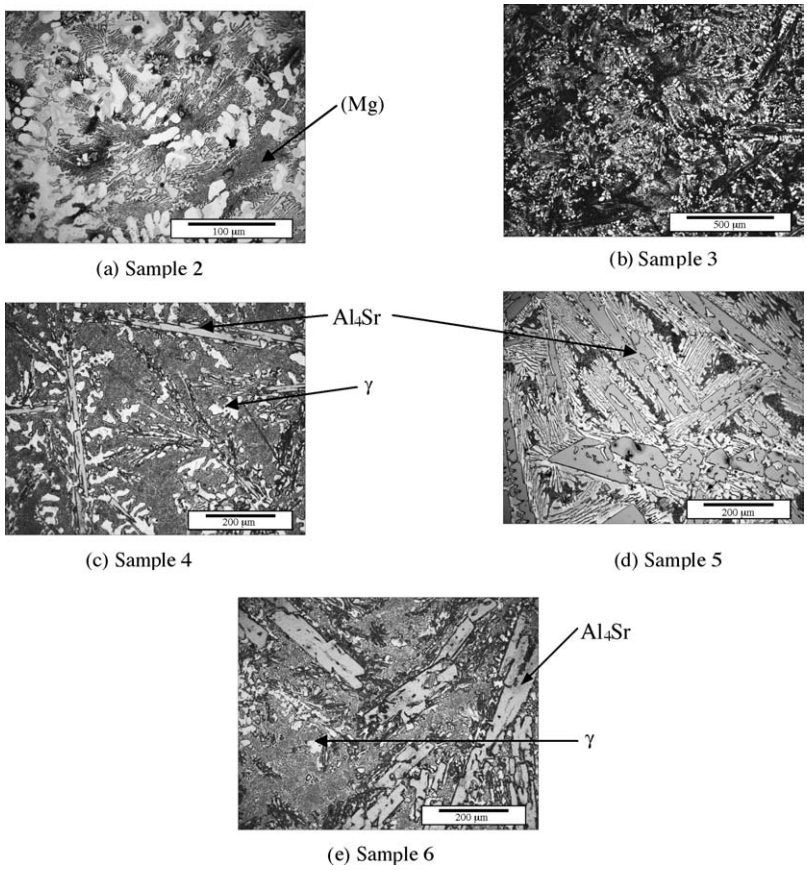

Fig. 5. Optical micrograph of samples (a) 2, (b) 3, (c) 4, (d) 5, and (e) 6.

as τ_2. Further investigation to identify the nature of the ternary phases in the Mg–Al–Sr system is being conducted in our group.

Table 4 shows the calculated transformation temperatures and associated reactions with DSC signals of samples 10–12. The number of transformations, predicted by the thermodynamics, matched well with the experimental results. Fig. 11 illustrates the microstructure of samples 10–12. Samples 10 and 11 appear to have a similar microstructure. From the analysis of XRD pattern and thermodynamics, it may be concluded that the light gray plate-like phase is Al_4Sr. Sample 12 gives a different microstructure, as can be seen in Fig. 11(c).

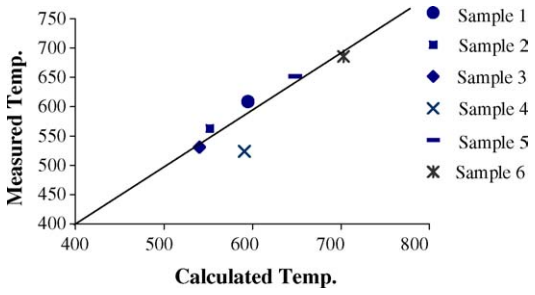

Fig. 6. Comparison between calculated and experimental DSC data.

This alloy is the far-most composition from Mg corner in this phase field, as can be seen in Fig. 1.

In the phase field of (Mg) + Al_2Sr + Al_4Sr, samples 13 and 14 have been identified positively with Al_2Sr and Al_4Sr along with some distinct unknown peaks. However, the unknown peaks for these two samples appeared in the same manner, as shown in Fig. 10(d) and (e), and tentatively designated as τ_3.

DSC spectra and phase assemblage diagram of sample 13, with heating and cooling runs, are shown in Fig. 12. For this sample, the liquidus temperature is observed during cooling as 677 °C. The size of the freezing signals increased due to supercooling.

3.3. *Samples in $Al_4Sr + \gamma + \beta$ phase field*

Three alloys in $Al_4Sr + \gamma + \beta$ phase field, as shown in Fig. 1, have been investigated. Fig. 13 shows that the DSC spectra of these alloys during heating are similar with a small variation in the thermal arrest of the second peak. Nevertheless, the DSC spectra showed that the invariant reaction for these samples occurred at close temperatures; 459, 453 and 452 °C, respectively. Fig. 14 shows the calculated vertical section in comparison with the DSC result from the cooling curve for sample 15. It can be seen from this figure that the two signals at higher temperature correspond to the calcu-

Table 2
DSC measurements with thermodynamic analysis of Mg–Al–Sr alloys (h denotes heating, and c denotes cooling)

Sample	DSC thermal signals	Thermodynamic calculation based on the database reported in [11]	
		Temperature (°C)	Reaction or phase boundary
1	609c	591	L/L + (Mg)
	596c/605h		
	517c/535h	535	L + (Mg)/(Mg) + Al_4Sr
		222	(Mg) + Al_4Sr/(Mg) + Al_4Sr + γ
2	563h	551	L/L + (Mg)
	531c	533	L + (Mg)/(Mg) + Al_4Sr
	516c/536h		
	510c/491h		
	427c/441h		
		282	(Mg) + Al_4Sr/(Mg) + Al_4Sr + γ
3	531c	540	L/L + (Mg) + Al_4Sr
	528c	530	L + (Mg) + Al_4Sr/(Mg) + Al_4Sr
	516c/523h		
	487c/510h		
	427c/442h		
		398	(Mg) + Al_4Sr/(Mg) + Al_4Sr + γ
4	524	591	L/L + Al_4Sr
	514c		
	472c		
	435c/494h	496	L + Al_4Sr/L + (Mg) + Al_4Sr
	422c/442	429	L + (Mg) + Al_4Sr/(Mg) + Al_4Sr + γ
5	652	648	L/L + Al_4Sr
	647c	535	L + Al_4Sr/L + (Mg) + Al_4Sr
	510c/513h	525	L + (Mg) + Al_4Sr/(Mg) + Al_4Sr
	453c/489h		
	431c/445h		
		318	(Mg) + Al_4Sr/(Mg) + Al_4Sr + γ
6	686c	703	L/L + Al_4Sr
	499c/490h	532	L + Al_4Sr/L + (Mg) + Al_4Sr
	448c/449h		
	432c	433	L + (Mg) + Al_4Sr/(Mg) + Al_4Sr + γ

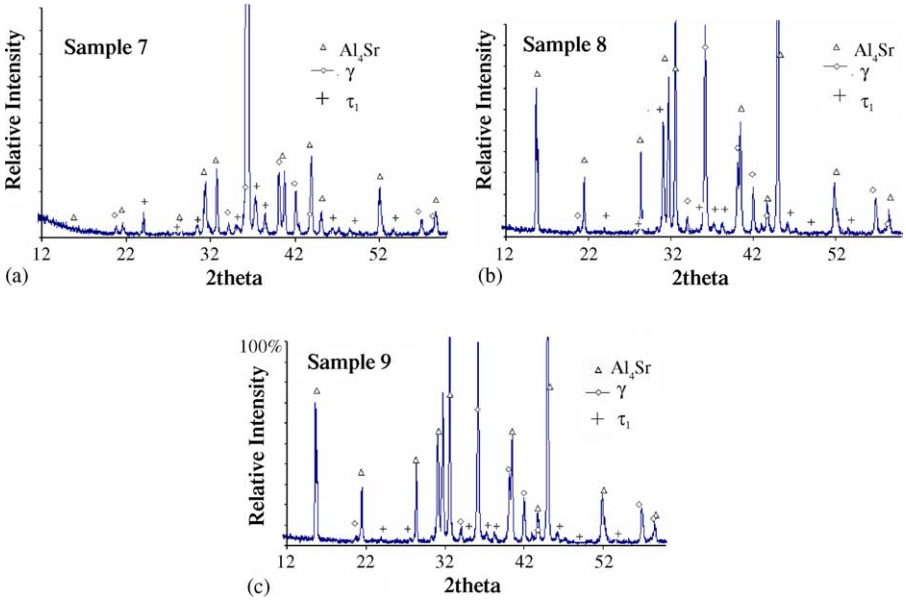

Fig. 7. XRD patterns of samples (a) 7 (13.02/46.92/40.06, Sr/Mg/Al, wt.%), (b) 8 (24/30/46, Sr/Mg/Al, wt.%), and (c) 9 (32/22/46, Sr/Mg/Al, wt.%).

Table 3
DSC measurements with thermodynamic analysis of Mg–Al–Sr alloys (h denotes heating, and c denotes cooling)

Sample	DSC thermal signals	Thermodynamic calculation based on the database reported in [11]	
		Temperature (°C)	Reactions or phase boundary
7	676	703	L/L + Al_4Sr
	510h	443	L + Al_4Sr/L + Al_4Sr + γ
	444c/466h	429	L + Al_4Sr + γ/(Mg) + Al_4Sr + γ
8	–	802	L/L + Al_4Sr
	507h		
	489h		
	445c/457h	446	L + Al_4Sr/L + Al_4Sr + γ
		427	L + Al_4Sr + γ/(Mg) + Al_4Sr + γ
9	–	846	L/L + Al_4Sr
	506h	501	L + Al_4Sr/L + Al_4Sr + (Mg)
	445c/457h	429	L + Al_4Sr + (Mg)/(Mg) + Al_4Sr + γ

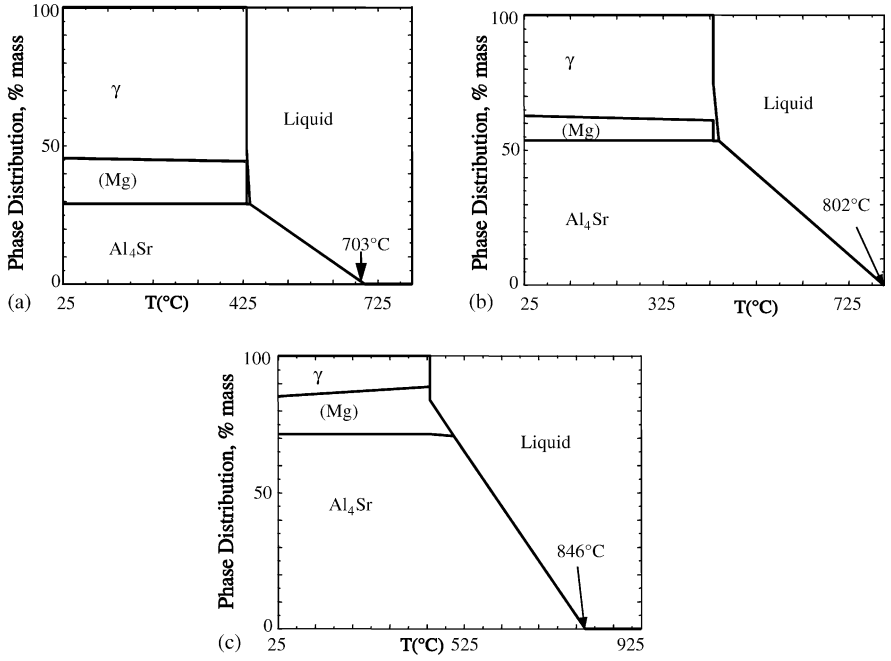

Fig. 8. Phase assemblage diagram of samples (a) 7, (b) 8, and (c) 9.

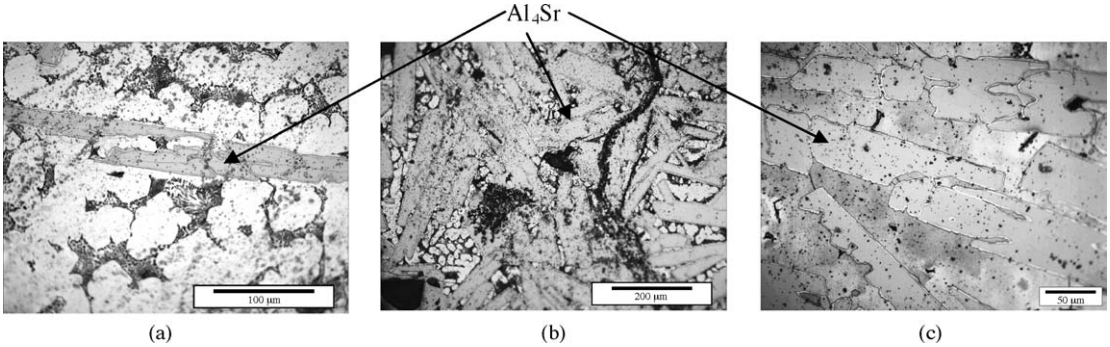

Fig. 9. Optical microscopic images of samples (a) 7, (b) 8, and (c) 9.

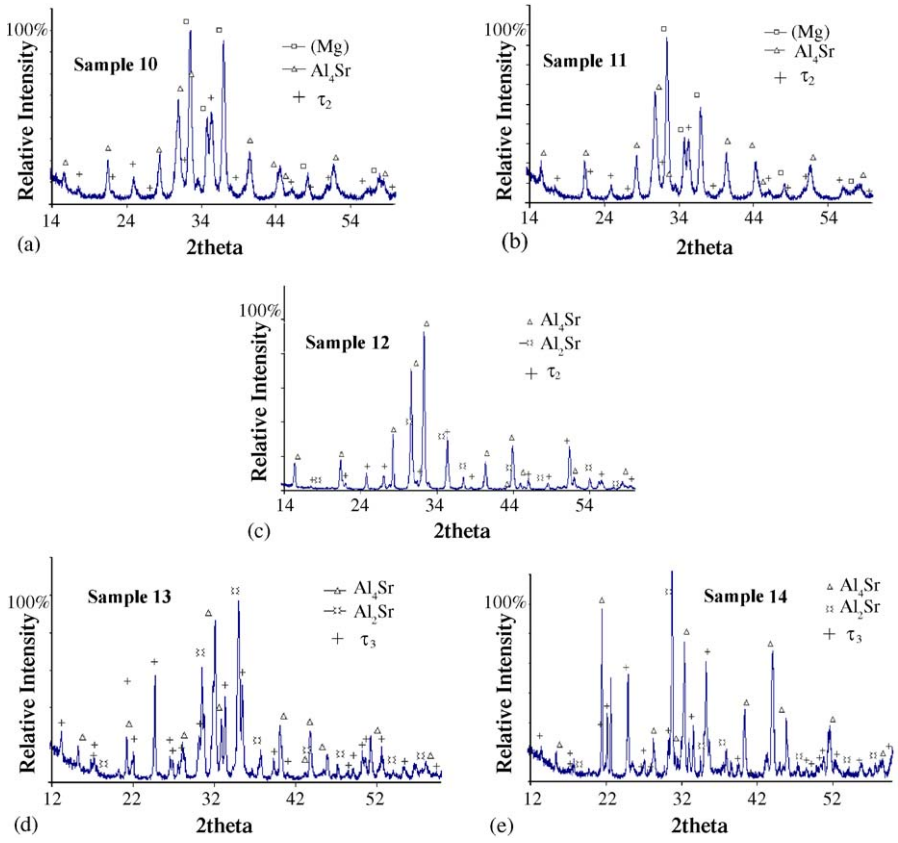

Fig. 10. XRD patterns of samples (a) 10 (22.78/54.39/22.83, Sr/Mg/Al, wt.%), (b) 11 (27.83/42.89/29.28, Sr/Mg/Al, wt.%), (c) 12 (48.30/19.26/32.44, Sr/Mg/Al, wt.%), (d) 13 (34.83/39.59/25.58, Sr/Mg/Al, wt.%), and (e) 14 (39.87/30.73/29.4, Sr/Mg/Al, wt.%).

lated diagram, but lower transformation temperature was not obtained by the DSC. The enthalpy of invariant reaction for samples 15–17 were registered as 316.67, 390 and 205.34 J/g, respectively.

It can be seen from Fig. 15 that samples 15–17 were identified with all the three phases predicted by the thermodynamic model, and γ has a very small volume fraction. β has a complex cubic unit cell (space group *Fm3m*, $a = 4.2155$ Å) [19]. Fig. 16 shows the optical micrograph of samples 15–17. The micrographs show different phase morphologies and the plate-like structure was designated as Al_4Sr.

3.4. Samples in (Al) + Al_4Sr + β phase field

Fig. 1 shows three samples that have been investigated in (Al) + Al_4Sr + β phase field. A DSC spectrum of sample 18 is shown in Fig. 17(a). Two samples reported by Makhmudov et al. [8] as ternary eutectic have been prepared. Among these samples, only sample 18 (4.56/31.63/63.81 Sr/Mg/Al wt.%) shows eutectic behavior, where the DSC heating and cooling runs reveal one single invariant reaction, as shown in Fig. 17(a). But the thermodynamic calculation of this sample, shown in Fig. 17(b), did not comply with the experimental

Table 4
DSC measurements with thermodynamic analysis of Mg–Al–Sr alloys (h denotes heating, and c denotes cooling)

Sample	DSC thermal signals	Thermodynamic calculation based on the database reported in [11]	
		Temperature (°C)	Reaction or phase boundary
10	618	605	L/L + Al_4Sr
	544c/560h	528	L + Al_4Sr/L + Al_4Sr + Mg
	513c/523h	494	L + Al_4Sr + Mg/Al_2Sr + Al_4Sr + Mg
11	571	664	L/L + Al_4Sr
	546c/561h	525	L + Al_4Sr/L + Al_4Sr + Mg
	513c/524h	496	L +Al_4Sr + Mg/Al_2Sr + Al_4Sr + Mg
12	643	783	L/L + Al_4Sr
	632h	716	L + Al_4Sr/L + Al_4Sr + Mg
	599c/615h	499	L + Al_4Sr + Mg/Al_2Sr + Al_4Sr + Mg

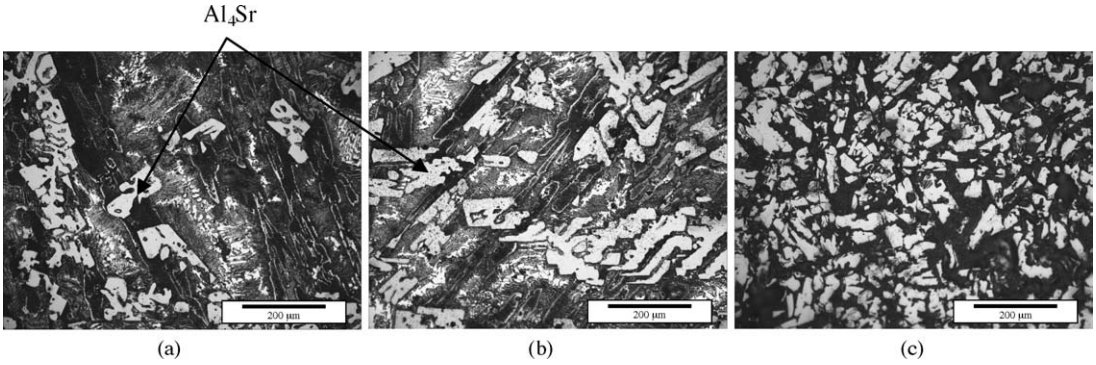

Fig. 11. Optical micrograph of samples (a) 10, (b) 11, and (c) 12.

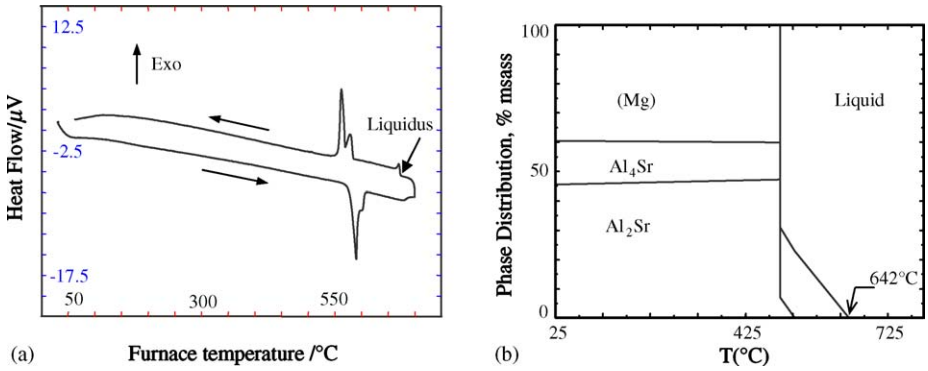

Fig. 12. (a) DSC spectra, (b) phase assemblage diagram of sample 13.

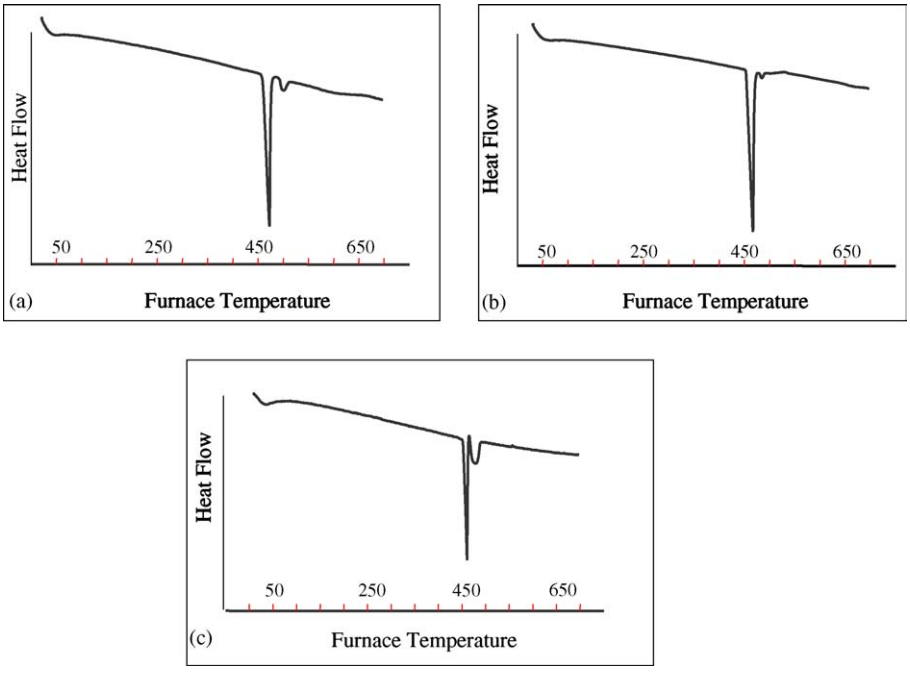

Fig. 13. DSC traces of the three samples: (a) 15, (b) 16, and (c) 17.

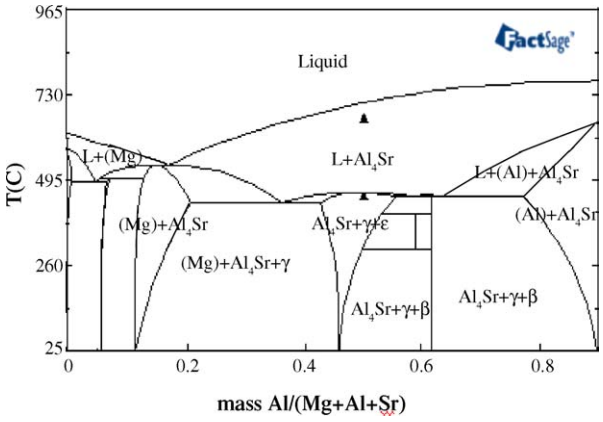

Fig. 14. Calculated vertical section at constant 9.5 wt.% Sr with DSC signals from cooling curve of sample 15.

result. The liquidus temperature of sample 19 is quite close to the calculated temperature, whereas the liquidus temperature and the number of transformations of sample 20 did not show good agreement with the thermodynamic predictions.

XRD patterns of samples 18–20 are shown in Fig. 18. The patterns were identified with three phases predicted by the thermodynamic calculations. Different microstructures were observed for these samples, and are shown in Fig. 19. It is very much apparent that the plate-like structure is Al_4Sr, since it was the common phase in most of the investigated samples and was detected in the XRD patterns for the three samples.

3.5. Samples in (Mg) + Al_2Sr + $Mg_{17}Sr_2$ phase field

Two samples have been prepared in this phase field, as shown in Fig. 1. DSC spectra and phase assemblage diagram of sample 22 are shown in Fig. 20. The DSC signal shows only one peak; hence, this composition is at the ternary eutectic point or very close to it. From the phase assemblage diagram, although all the three phases did not precipitate at the same temperature, this diagram shows that sample 22 is indeed close to the eutectic composition, and thus, matches with the DSC result. The enthalpy of melting for this sample was registered as 300 J/g. Sample 21 has been identified with all the three phases predicted by the thermodynamics, as shown in

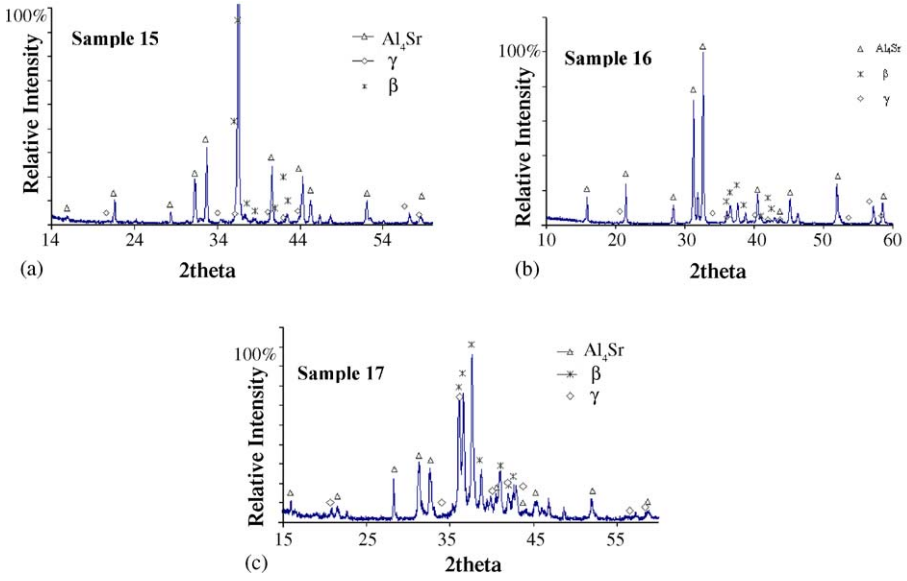

Fig. 15. XRD pattern of samples (a) 15 (9.5/40/50.5, Sr/Mg/Al, wt.%), (b) 16 (11/30/59, Sr/Mg/Al, wt.%), and (c) 17 (31.18/14.42/54.4, Sr/Mg/Al, wt.%).

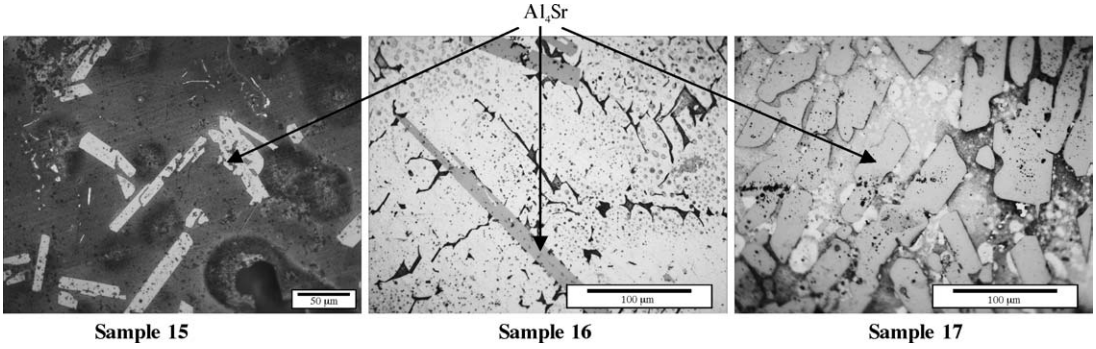

Fig. 16. Optical micrograph of samples (a) 15, (b) 16, and (c) 17.

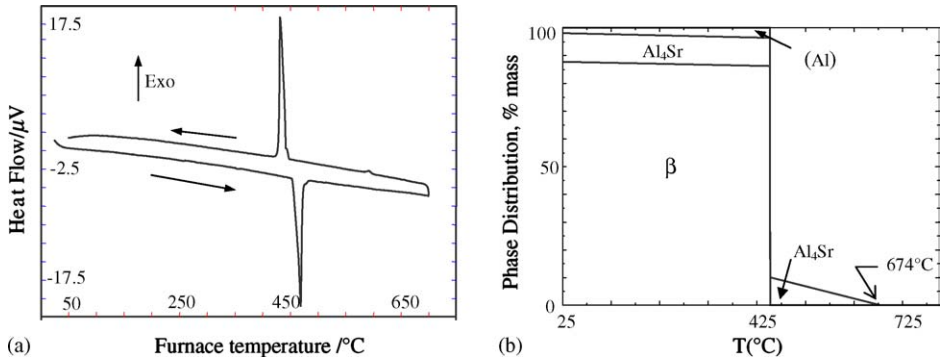

Fig. 17. (a) DSC spectra of sample 18 (4.56/31.63/63.81, Sr/Mg/Al, wt.%) during heating and cooling, and (b) phase assemblage diagram of sample 18.

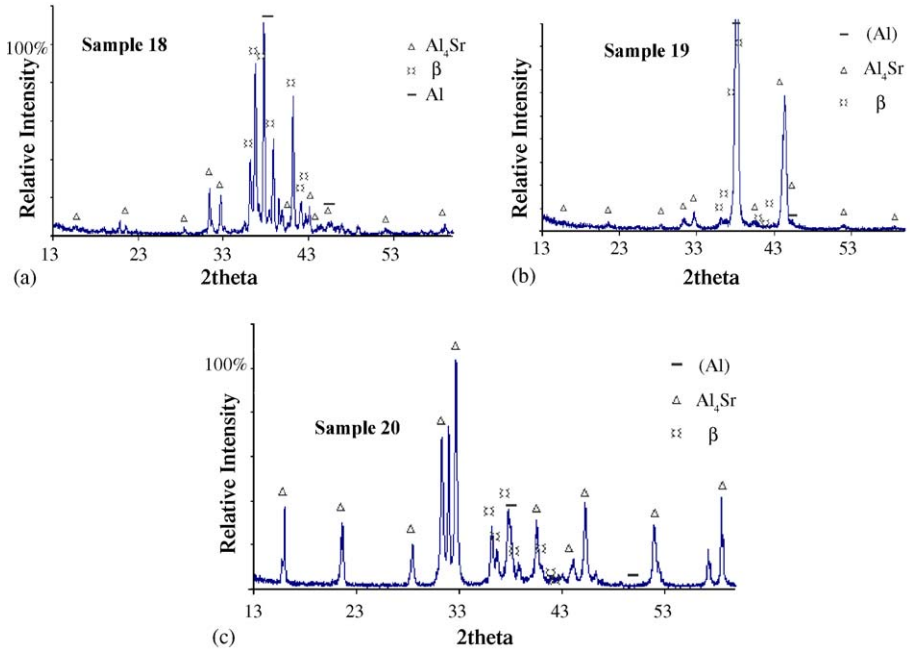

Fig. 18. XRD pattern of samples (a) 18 (4.56/31.63/63.81, Sr/Mg/Al, wt.%), (b) 19 (2.04/10.80/87.16, Sr/Mg/Al, wt.%), and (c) 20 (23/15/62, Sr/Mg/Al, wt.%).

Fig. 21(a). However, sample 22 has been identified positively with only two phases: (Mg) and $Mg_{17}Sr_2$, and the sample did not contain Al_2Sr. Instead, there are some unknown peaks that do not match with any known binary phase in the Mg–Al–Sr system; therefore, these new peaks are identified tentatively as a new ternary phase τ_4. $Mg_{17}Sr_2$ was identified using a hexagonal unit cell (space group $P6_3/mmc$, $a = 10.535$ Å, $c = 10.356$ Å) [19]. In this study, it was observed that it is very difficult to identify the Al_2Sr compound. This suggests that perhaps Al_2Sr forms a solid solution with other species in the

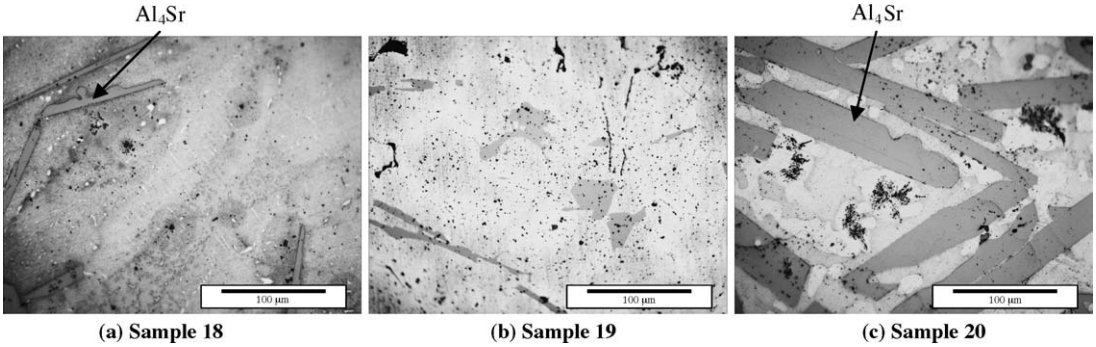

Fig. 19. Optical micrograph of samples (a) 18, (b) 19, and (c) 20.

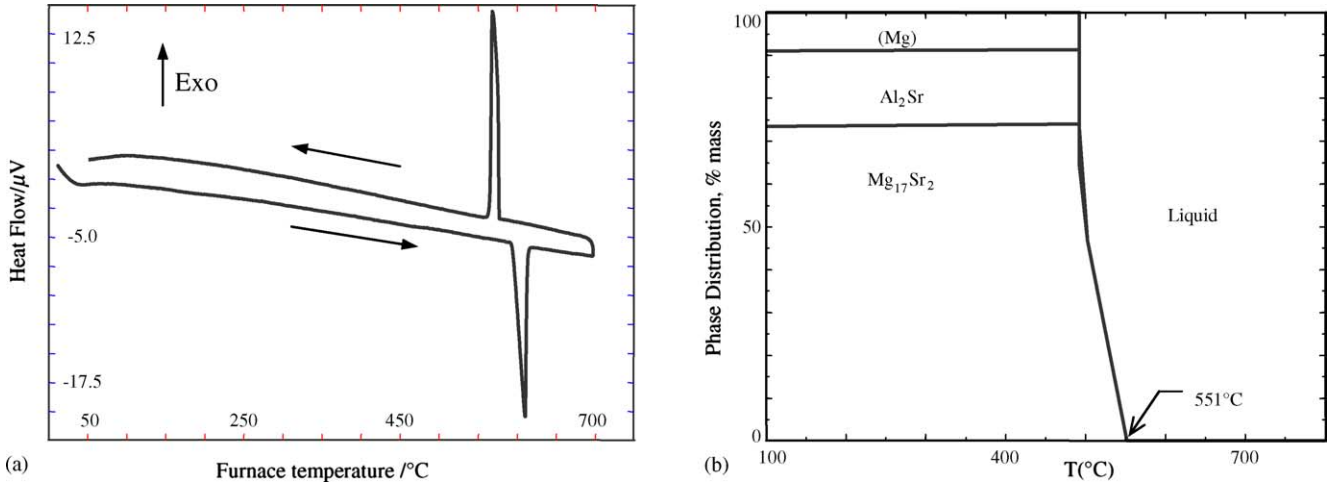

Fig. 20. (a) DSC spectra, and (b) phase assemblage diagram of sample 22.

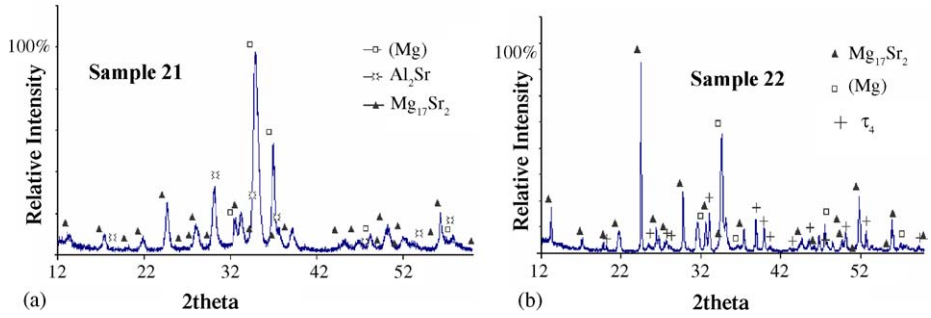

Fig. 21. X-ray diffraction pattern of samples (a) 21 (19.90/72/8.1, Sr/Mg/Al, wt.%), and (b) 22 (32.74/60.55/6.71, Sr/Mg/Al, wt.%).

Mg–Al–Sr system. Even though these two samples belong to the same phase field, different microstructures were observed as shown in Fig. 22.

3.6. Microstructural evolution

The microstrutural evolution was observed by comparing the microstructure of the as-cast with the post-DSC samples for five different compositions. In the as-cast condition, sample 1 has primary (Mg) phase and network of grain boundary phase, as shown in Fig. 23(a). It can be seen from Fig. 23(b) that the morphology and the network nature of the grain boundary phase experienced changes during the heat treatment. The network has become less complete and the grain size has increased after the heat treatment. The microstructure of sample 4, shown in Fig. 23(c), is charac-

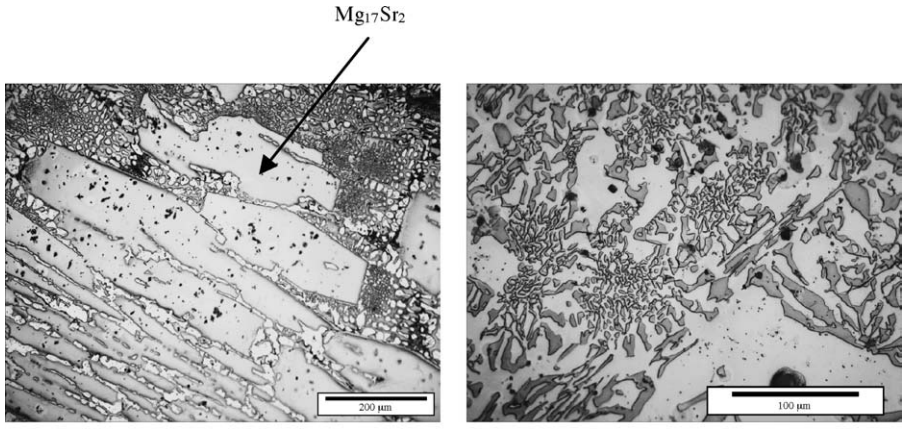

(a) Sample 21 (b) Sample 22

Fig. 22. Optical micrograph of samples (a) 21, and (b) 22.

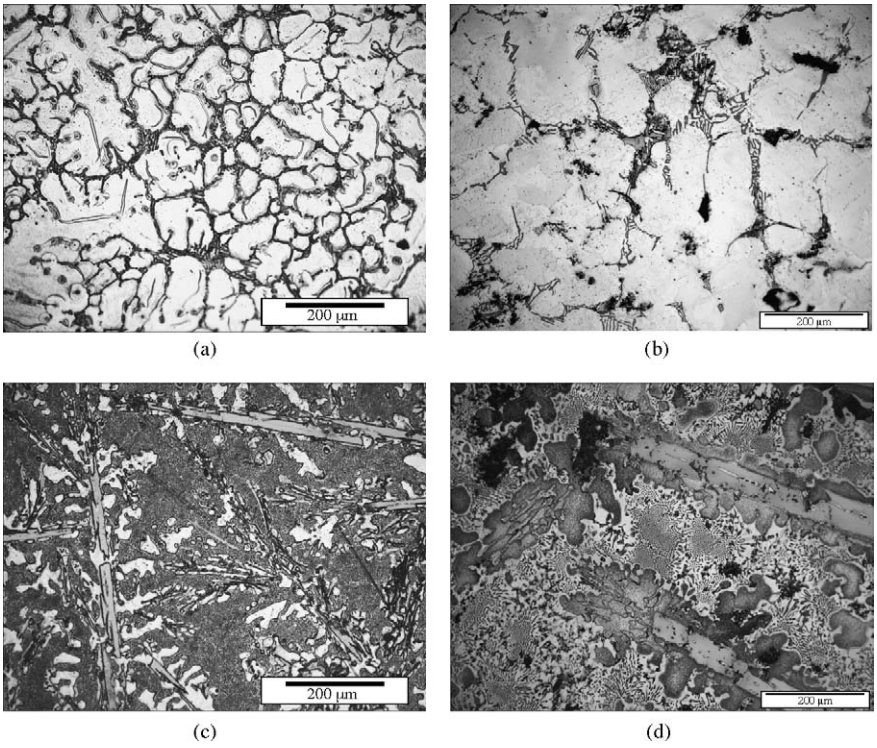

Fig. 23. Optical micrograph of sample 1: (a) as-cast condition, (b) post-DSC condition; optical micrograph of sample 4: (c) as-cast condition, (d) post-DSC condition.

terized as a dendritic microstructure, which has Al_4Sr as the primary phase. Post-DSC sample shows that the intermetallic has grown and the eutectic morphology is more evident. The same phenomena was observed in the other investigated alloys.

Fig. 24 shows the ternary phase diagram of the Mg–Al–Sr system, where four new phase fields have been identified using XRD, metallography and DSC.

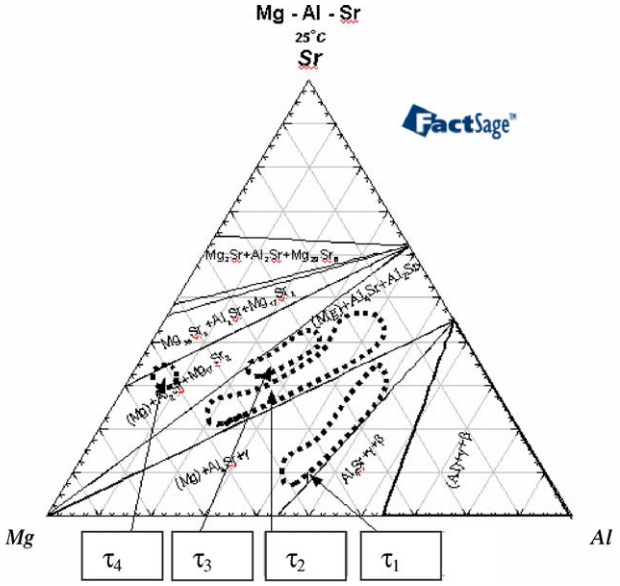

Fig. 24. New tentative phase fields in the Mg–Al–Sr system.

4. Conclusion

A comprehensive study using DSC, XRD and metallography on the ternary equilibria in the Mg–Al–Sr system was conducted. Four new phase fields were found in this system which may be due to new ternary solid solutions or compounds. Other ternary phases claimed by Makhmudov et al. were not observed in this investigation. Al_4Sr and (Mg) were found to be the dominating phases in the investigated alloys. The identified phases in the as-cast condition were found consistent and thermodynamically stable with the post-DSC samples in the five investigated alloys. The experimental results were compared with the pertinent thermodynamic findings. Considerable disagreement between the thermodynamic model and the results of this study suggests that the Mg–Al–Sr system should be remodeled in light of the new experimental findings.

Acknowledgements

This research was carried out with the support of NSERC and NATEQ grants, Canada. The authors wish to express their appreciation for this support.

References

[1] R. Gradinger, P. Stolfig, Proc. Mine. Metals Mater. Soc. (TMS) (2003) 231–236.

[2] S. Das, JOM 55 (11) (2003) 22–26.
[3] M. Pekguleryuz, E. Baril, P. Labelle, D. Argo, J. Adv. Mater. 35 (3) (2003) 32–38.
[4] A. Prince, N. Nikitina, in: G. Petzow, G. Effenberg (Eds.), Ternary Alloys: A Comprehensive Compendium of Evaluated Constitutional Data and Phase Diagrams, vol. 16, VCH, New York, pp. 413–425.
[5] M.M. Makhmudov, A.V. Vakhovob, T.D. Dzhuraev, I.N. Ganiev, Dokl. Akad. Nauk Tadzh. 23 (1980) 25–28.
[6] M.M. Makhmudov, A.V. Vakhovob, T.D. Dzhuraev, Dokl. Akad. Nauk Tadzh. 24 (7) (1981) 435–438.
[7] M.M. Makhmudov, A.V. Vakhovob, T.D. Dzhuraev, Russ. Metall. 6 (1981) 209–212.
[8] M.M. Makhmudov, A.V. Vakhovob, T.D. Dzhuraev, Russ. Metall. 1 (1982) 122–124.
[9] M.M. Makhmudov, A.V. Vakhovob, I.N. Ganiev, Zavod. Lab. 48 (10) (1982) 61–62.
[10] E. Baril, P. Labelle, M. Pekguleryuz, JOM 55 (11) (2003) 34–39.
[11] P. Chartrand, A.D. Pelton, J. Phase Equilibria 5 (6) (1994) 591–605.
[12] O. Koray, PhD Thesis, The Pennsylvania State University, 2004.
[13] Z.K. Liu, Y. Zhong, C. Wolverton, A.Y. Chang, Acta Mater. 52 (9) (2004) 2739–2754.
[14] M.A. Parvez, E. Essadiqi, M. Medraj, Proc. CSME Forum (2004) 829–838.
[15] X. Wang, M.A. Parvez, E. Essadiqi, M. Medraj, Proc. CSME Forum (2004) 819–828.
[16] W. Kraus, G. Nolze, PowderCell for Windows, 1999.
[17] M.A. Parvez, X. Wang, E. Essadiqi, M. Medraj, Proc. Mine. Metals Mater. Soc. (TMS) (2005) 179–184.
[18] FactSage 5.3, http://www.factsage.com, 2004.
[19] P. Villars, Pearson's Handbook, ASM International, 1997.